Journal of Quantitative Spectroscopy & Radiative Transfer 185 (2016) 12–21

Contents lists available at ScienceDirect

Journal of Quantitative Spectroscopy & Radiative Transfer

journal homepage: www.elsevier.com/locate/jqsrt

First high resolution analysis of the $2\nu_1$, $2\nu_3$, and $\nu_1 + \nu_3$ bands of $S^{18}O_2$

O.N. Ulenikov [a,*], E.S. Bekhtereva [a], O.V. Gromova [a], V.A. Zamotaeva [a], E.A. Sklyarova [a], C. Sydow [b], C. Maul [b], S. Bauerecker [b]

[a] Institute of Physics and Technology, National Research Tomsk Polytechnic University, Tomsk 634050, Russia
[b] Institut für Physikalische und Theoretische Chemie, Technische Universität Braunschweig, D-38106 Braunschweig, Germany

ARTICLE INFO

Article history:
Received 21 July 2016
Received in revised form
12 August 2016
Accepted 12 August 2016
Available online 21 August 2016

Keywords:
$S^{18}O_2$ sulfur dioxide
High-resolution spectra
Spectroscopic parameters

ABSTRACT

We report the results of a highly accurate, $(1–3)\times 10^{-4}$ cm^{-1}, ro-vibrational analysis of the $S^{18}O_2$ molecule in the spectral region of 2100–2700 cm^{-1}. More than 2910, 2130, and 1390 transitions belonging to the $2\nu_1$, $\nu_1+\nu_3$, and $2\nu_3$ bands were assigned for the first time with the values of quantum numbers $J^{max.}/K_a^{max.}$ equal to 67/26, 81/25 and 53/16, respectively. The weighted fit of experimentally assigned transitions was made with the Hamiltonian model which takes into account Coriolis resonance interactions between the vibrational states $(v_1v_2v_3)$ and $(v_1 \mp 1 v_2 v_3 \pm 1)$ and Fermi interactions between the states $(v_1v_2v_3)$ and $(v_1 \mp 1 v_2 \pm 2 v_3)$. To make the ro-vibrational analysis physically more suitable, the initial values of main spectroscopic parameters have been estimated theoretically. Finally, the set of 43 spectroscopic parameters obtained from the fit reproduces values of 2384 initial "experimental" ro-vibrational energy levels (more than 6430 transitions assigned in the experimental spectra) with the $rms = 1.74\times 10^{-4}$ cm^{-1}.

1. Introduction

In this paper we continue our recent work, Refs. [1–8], of the analysis of high resolution rotation–vibration spectra of sulfur dioxide and its isotopologues, which is an important topic in many fields such as chemistry, interstellar space, planetary nebulae, study of atmospheres of the Earth and Venus (where the abundance of sulfur dioxide is a million times higher than in the Earth's atmosphere), food technology, and laser techniques. It plays a significant role as a pollutant in the terrestrial atmosphere. In particular, sulfur dioxide is one of the major air pollutants released in the atmosphere as a result of volcanic eruptions and of fuel combustion in human activities; it contributes to the generation of smog and constitutes a serious health hazard for the respiratory system (see, *e.g.*, Refs. [9–16]). To solve the problems of propagation of monochromatic radiation in the atmosphere, laser sounding, information transfer, the remote detection and monitoring of SO_2 in situ, etc., one also should have a good knowledge of the fine structure of the SO_2 absorption spectra in different parts of the electromagnetic spectrum, in particular, in the infrared. For this reason, numerous spectroscopic studies of the sulfur dioxide molecule have been performed during many years as well in the microwave, submillimeter wave and infrared regions (extensive list of references to earlier studies of sulfur dioxide spectra can be found, *e.g.*, in Ref. [17]; see also Ref. [18]).

The present study focuses on the spectroscopic analysis of the $S^{18}O_2$ isotopologue of sulfur dioxide in the region of the $2\nu_1$, $\nu_1+\nu_3$ and $2\nu_3$ absorbtion bands. Up to now,

* Corresponding author.
E-mail address: Ulenikov@mail.ru (O.N. Ulenikov).

http://dx.doi.org/10.1016/j.jqsrt.2016.08.008
0022-4073/

the high resolution spectra of $S^{18}O_2$ have been analyzed only in a few reports [19–24]. While the $2\nu_1$, $\nu_1+\nu_3$ and $2\nu_3$ bands of sulfur dioxide have been discussed in Refs. [25–38] for $^{32}S^{16}O_2$ and $^{34}S^{16}O_2$, an analysis is still missing for the $S^{18}O_2$ isotopologue.

2. Experimental details

The $S^{18}O_2$ sample gas was produced by controlled combustion of pure sulfur in naturally isotopic composition (Roth, $>99.999\%$) in $^{18}O_2$ (Sigma-Aldrich, 99 at%). Impurities of $^{16}O_2$ in the sample lead to detectable portions of $S^{16}O^{18}O$ and $S^{16}O_2$ in the spectra. The details of the procedure are described in our preceding work, Ref. [23]. In the spectral region between 1800 and 2800 cm^{-1} two spectra have been recorded with a Bruker IFS120HR Fourier transform infrared spectrometer by use of a stainless steel White cell of one meter base length which was adjusted at 4 and 24 m optical pathlength. A globar radiation source (driven at 24 V, 3.8 A and about 1 Pa N_2 atmosphere), KBr windows, a KBr beamsplitter and a mercury–cadmium–telluride (MCT) semiconductor detector have been used for recording the spectra. The whole spectrometer was pumped by a turbomolecular pump to an average pressure below 0.1 Pa. The transmission spectrum was obtained by division of the highly resolved single-channel spectrum by a background spectrum with a lower resolution of 0.1 cm^{-1} (averaged by 200 scans). Using Norton-Beer weak apodization the nominal optical resolution was 0.0025 cm^{-1} for both spectra, defined by $0.9\times 1/d_{MOPD}$ (maximum optical path difference) which leads to an instrumental linewidth of 0.002 cm^{-1}. The Doppler broadening for $^{32}S^{18}O_2$ at 298.15 K was between 0.0027 cm^{-1} (at 1800 cm^{-1}) and 0.0042 cm^{-1} (at 2800 cm^{-1}). The pressure broadening was 0.00003 and 0.0005 cm^{-1} at the used pressures of 10 and 150 Pa. This means that it has a minor contribution to the total line widths which result between 0.0034 and 0.0047 cm^{-1} (root sum square approximation of convolution) and which is in accordance with the experimental results. The spectra were calibrated with N_2O lines at a partial N_2O pressure of about 10 Pa. For optimization of data recording and line calibration we used procedures described in Refs. [39,40].

3. Description of the spectra and assignment of transitions

The survey spectra I and II in the region of 2100–2700 cm^{-1}, where the $2\nu_1$, $\nu_1+\nu_3$ and $2\nu_3$ bands of the $S^{18}O_2$ molecule are located, are shown in Fig. 1. As mentioned in the Experimental section, the absorption bands of $S^{16}O_2$ and of $S^{16}O^{18}O$ are also present in the spectrum. One also can see strong absorption which is caused by $C^{16}O_2$, $C^{18}O_2$, and $C^{16}O^{18}O$ (middle part of Fig. 1) and by $C^{18}O$ and $C^{16}O$ (left part of Fig. 1). The P- and R-branches of the bands $\nu_1+\nu_3$ (which is the strongest band with the center close to 2407 cm^{-1}) and $2\nu_1$ (band center is near 2196 cm^{-1}) of $S^{18}O_2$ are clearly pronounced in both spectra I and II. The weak $2\nu_3$ band (band center is near 2627 cm^{-1}) can only be seen in spectrum II. From Fig. 1,

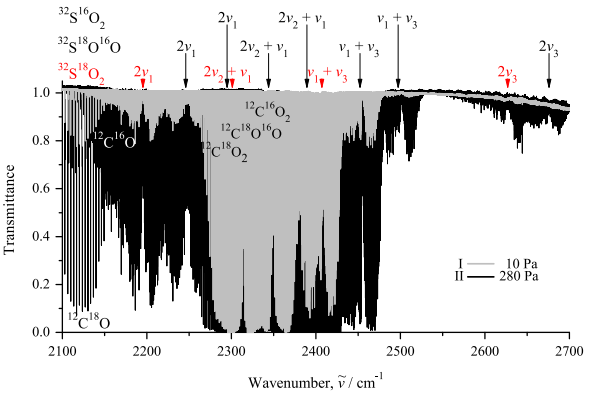

Fig. 1. Survey spectrum of $S^{18}O_2$ in the region of 2100–2700 cm^{-1}. Experimental conditions: absorption path lengths are 4 and 24 m; room temperature; number of scans and sample pressure is 1080 and 10 Pa for spectrum I and 580 and 280 Pa for spectrum II. The corresponding bands of $S^{16}O_2$ and of $S^{16}O^{18}O$ are also present and marked in Fig. 1. In the central and left part of the figure, one can see bands of $C^{16}O_2$, $C^{18}O_2$, $C^{16}O^{18}O$, $C^{18}O$, and $C^{16}O$.

one can also get an idea on relative intensities of the bands $\nu_1+\nu_3$, $2\nu_1$ and $2\nu_3$. To illustrate the quality of experimental results, the top parts of Figs. 2–4 show small fragments of high-resolution spectra in the region of the Q-branches of the $\nu_1+\nu_3$, $2\nu_1$ and $2\nu_3$ bands, respectively. The structures of the Q-branches are clearly pronounced, and we would like to attract the reader's attention to Fig. 3 where two sets of the $^PQ_5(J)$ transitions of the $2\nu_1$ band are shown. One of them (odd values of quantum number J) shows a traditional behavior with "red" degrading. The second set of transitions (even values of quantum number J) demonstrates abnormal behavior which can be explained by the ratio between values of parameters C, Δ_J, and H_J (as the analysis showed, resonance interactions cannot be considered as a reason of discussed behavior of the $^PQ_5(J)$ transitions).

The $^{32}S^{18}O_2$ molecule is an asymmetric top of C_{2v} symmetry with the asymmetry parameter $\kappa=(2B-A-C)/(A-C)\approx -0.948$. On this reason, its three vibrational modes have the following symmetry: $q_\lambda\in A_1$ for $\lambda=1, 2$, and $q_\lambda\in B_1$ for $\lambda=3$. The rotational operators J_α and $k_{z\alpha}$ ($\alpha=x,y,z$) are transformed in the A-reduction and I^r representation in accordance with the following irreducible representations of the C_{2v} symmetry group (see, e.g., Refs. [41–44]): J_x and $k_{zx}\in B_2$; J_y and $k_{zy}\in B_1$; J_z and $k_{zz}\in A_2$. In consequence, bands of the two types are allowed in absorption from the ground vibrational state, Refs. [45,46]: parallel (or A_1) type bands which correspond to the vibrational transitions $(\nu_{A_1})\leftarrow(\nu_{gr.})$, and perpendicular (or B_1) type bands which correspond to the vibrational transitions $(\nu_{B_1})\leftarrow(\nu_{gr.})$. The selection rules for transitions in the parallel bands are

$$\Delta J=0,\pm 1,\quad \Delta K_a=even,\quad \Delta K_c=odd.$$

In turn, the selection rules for transitions in the perpendicular bands are

$$\Delta J=0,\pm 1,\quad \Delta K_a=odd,\quad \Delta K_c=odd.$$

Also, it is necessary to take into account that, due to nuclear spin statistics of the $^{32}S^{18}O_2$ molecule, only such $(J'K'_aK'_c)$ rotational states of the ground vibrational state are realized which satisfy the condition "the value of $(K'_aK'_c)$ is even".

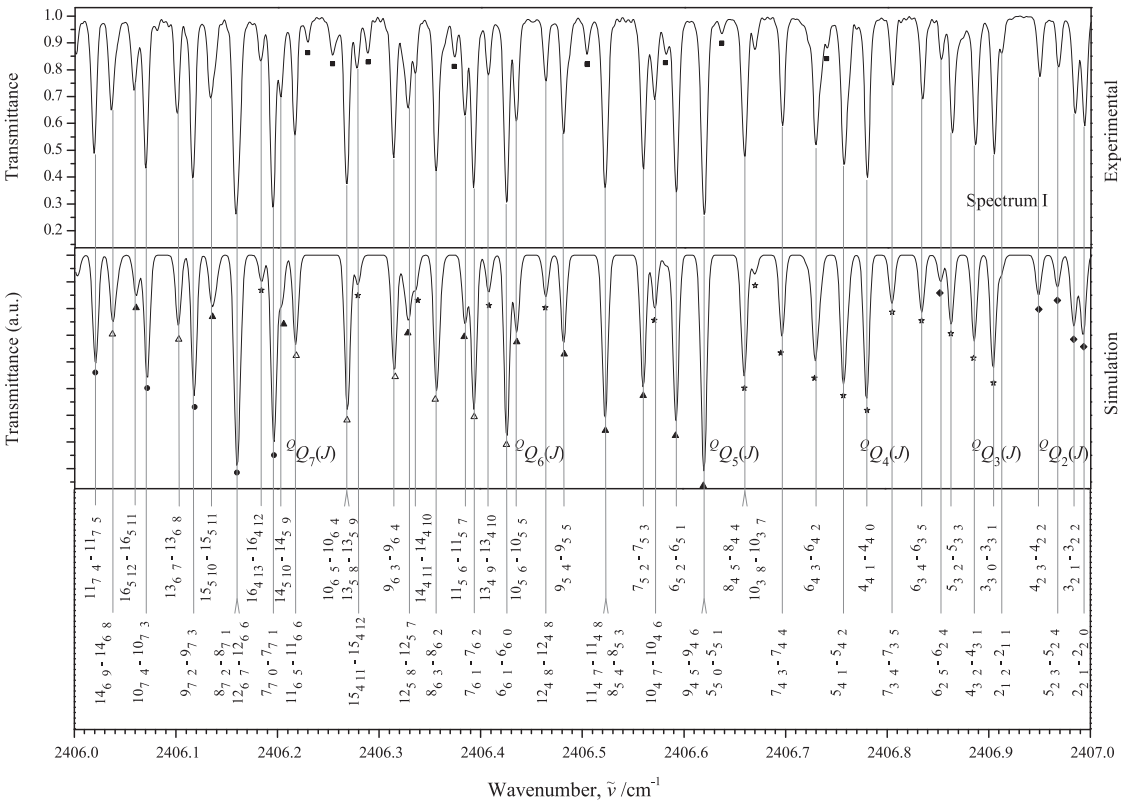

Fig. 2. Small part of the high resolution spectrum I (upper trace) of $S^{18}O_2$ in the region of the Q-branch of the $\nu_1+\nu_3$ band. For the experimental conditions see Table 1 and caption of Fig. 1. The lower trace is the simulated spectrum (see text for details). Some sets of assigned $^{Q}Q_{K_a}(J)$ transitions are marked in the simulated spectrum by dark and open triangles, dark and open stars and dark diamonds. Some unassigned lines, which are marked in the experimental spectrum by the dark squares, probably belong to the hot $\nu_1+\nu_2+\nu_3-\nu_2$ band of $S^{18}O_2$, or to the cold bands of other sulfur dioxide isotopic species.

Rotational states, which would correspond the condition ($J'K'_aK'_c$), are not realized.

The assignment of the transitions was made on the basis of the Ground State Combination Differences method. Here, the ground state rotational energies have been calculated with the parameters from Ref. [23]. As a result, more than 2910, 2130, and 1390 transitions with the values of quantum numbers $J^{max.}/K_a^{max.}$ equal to 67/26, 81/25 and 53/16 were assigned to the bands $2\nu_1$, $\nu_1+\nu_3$ and $2\nu_3$ (for more details, see statistical information in Table 2). The list of assigned transitions is presented in the Supplementary Materials section.

4. Hamiltonian model and estimation of spectroscopic parameters

4.1. Effective Hamiltonian

In the present study we took into account the fact that for the C_{2v}-symmetry species of the sulphur dioxide molecule, the Fermi-type interactions between the $(v_1v_2v_3)$ and $(v_1\mp1v_2\pm2v_3)$ vibrational states should be considered which is well known in the literature (see, *e.g.*, Refs. [34,47]). Also we followed the procedure of our preceding studies of the high resolution spectra of the $^{32}S^{16}O_2$ and $^{32}S^{18}O_2$ species and took the Coriolis-type interactions between the $(v_1v_2v_3)$ and $(v_1\mp1v_2v_3\pm1)$ vibrational states into account. As a consequence, in the theoretical analysis of the experimental data we used the Hamiltonian model which respects the presence of resonance interactions. Such Hamiltonian model was discussed in the preceding literature (see, *e.g.*, Refs. [48–50]). For that reason we reproduce it here without detailed explanations:

$$H^{v.-r.}=\sum_{v,\tilde{v}}|v\rangle\langle\tilde{v}|H_{v\tilde{v}}, \tag{1}$$

where the summation extends over all (in our case, six) interacting vibrational states: $|1\rangle\equiv(040,A_1)$, $|2\rangle\equiv(120,A_1)$, $|3\rangle\equiv(200,A_1)$, $|4\rangle\equiv(002,A_1)$, $|5\rangle\equiv(021,B_1)$ and $|6\rangle\equiv(101,B_1)$. The diagonal operators H_{vv} describe unperturbed rotational structures of the corresponding vibrational states. The nondiagonal operators $H_{v\tilde{v}}$ $(v\neq\tilde{v})$ describe resonance interactions (Fermi, or Coriolis) between the states $|v\rangle$ and $|\tilde{v}\rangle$. The diagonal block operators have the same form for all six vibrational states involved (Watson's Hamiltonian in the *A*-reduction and I^r representation), see, *e.g.*, Refs. [51,52]:

$$\begin{aligned}H_{vv}=E^v&+[A^v-\tfrac{1}{2}(B^v+C^v)]J_z^2+\tfrac{1}{2}(B^v+C^v)J^2+\tfrac{1}{2}(B^v-C^v)J_{xy}^2\\&-\Delta_K^vJ_z^4-\Delta_{JK}^vJ_z^2J^2-\Delta_J^vJ^4-\delta_K^v[J_z^2,J_{xy}^2]_+-2\delta_J^vJ^2J_{xy}^2+H_K^vJ_z^6\\&+H_{KJ}^vJ_z^4J^2+H_{JK}^vJ_z^2J^4+H_J^vJ^6+[J_{xy}^2,h_K^vJ_z^4+h_{JK}^vJ^2J_z^2+h_J^vJ^4]_+\\&+L_K^vJ_z^8+L_{KKJ}^vJ_z^6J^2+L_{JK}^vJ_z^4J^4+L_{KJJ}^vJ_z^2J^6+L_J^vJ^8\\&+\left[J_{xy}^2,l_K^vJ_z^6+l_{KJ}^vJ^2J_z^4+l_{JK}^vJ^4J_z^2+l_J^vJ^6\right]_+\\&+P_K^vJ_z^{10}+P_{KKKJ}^vJ_z^8J^2+P_{KKJJ}^vJ_z^6J^4+P_{JJK}^vJ_z^4J^6\end{aligned}$$